ORIGINAL RESEARCH PAPER
Pages: 328-343

A Fast Automatic Modulation Classification Based on STFT Using Hybrid Deep Neural Network

Ashwagh N[1]. Hassan, M[1]. Mohassel Feghhi[1*], and V. Esmaeili[1]
Faculty of Electrical and Computer Engineering University of Tabriz, Tabriz, Iran
ashwaqnama@tabrizu.ac.ir, mohasselfeghhi@tabrizu.ac.ir, v.esmaeili@tabrizu.ac.ir
Corresponding author: mohasselfeghhi@tabrizu.ac.ir

DOI:10.22070/JCE.2023.17933.1250

Abstract- Automatic modulation classification is used in various applications, including satellite communication systems, military communication, and submarine communications. In this paper, the automatic classification of modulation types is done using a two-stage method that combines a short-time Fourier transform (STFT) and a hybrid deep neural network (HDNN). At the first stage, using the STFT as a data source, the time-frequency information is retrieved from the modulated signals. A hybrid deep neural network feed two-dimensional (2D) images as inputs. In the second stage, the HDNN feeds the 2D time-frequency data to classify the various modulation types. Six various types of modulation schemes, including amplitude-shift keying, frequency-shift keying, phase-shift keying, quadrature amplitude-shift keying, quadrature frequency-shift keying, and quadrature phase-shift keying, are recognized automatically in the SNR range of 0 to 25 dB. An exhaustive computer simulation has been performed to evaluate the performance of the proposed digital modulation classification method. The simulation results show that, in comparison with the existing methods, our proposed method performs well and significantly reduces the processing time.

Index Terms- Classification, hybrid deep neural network, modulation, short-time Fourier transform.

I. INTRODUCTION

The variety of modulation schemes utilized in the wireless transmission systems is increasing. Therefore, quickly and automatically analyzing and classifying communication signals is necessary [1]-[2]. Automatic modulation classification (AMC), as a intermediate stage in blind signal processing, is an essential approach for detecting modulation types for software-defined radio and Cognitive Radio (CR) [3]. Also, the AMC has a wide application both in the military and civil areas.

For the AMC, two types of classifiers are presented, namely, conventional and deep learning based

Manuscript received 15-March-2021 and revised 11-May-2021, *P-ISSN: 2322-4088*
Accepted on 13- June-2021 *E-ISSN:2322-3936*

AMC [4]-[5]. The first type contains the feature-based (FB) and the likelihood-based (LB) methods. The LB method classifies the incoming signals by computing their probability function under several alternative hypotheses and comparing the outcomes with a specified threshold to determine possible categories of received signals. The LB method calculates the likelihood ratios of the received signals under different hypotheses to minimize the probability of misclassification. When all the parameters except the modulation type are given, the LB approaches are the optimal methods in the Bayesian sense. Otherwise, these approaches suffer from the intensive computations and high sensitivity to non-ideal channel conditions or unknown parameters [6]-[7].

The suboptimal FB approaches are presented with less computational complexity. In these approaches, the modulation type is determined by analyzing the characteristics of the received signals. Although the performance of the LB approach is affected by timing errors and phase errors, it can theoretically reach an optimal solution when the complexity increases. Nevertheless, the performance of the FB approach is suboptimal, but real-time implementation is possible. The high-quality features can achieve high performance at the least cost. These features have been addressed in the literature, such as the wavelet transform (WT) [8], the cyclostationarity [9], and the higher-order cumulants [10]. Also, cyclic cumulants [11] and cumulants [12] techniques have also been used for feature extraction. These features are sent as input to the FB classifiers such as the Random Forests (RF) [13], the K-Nearest Neighbor (KNN) [14], the Support Vector Machine (SVM), and the Gaussian Naive Bayes (GNB) [15]-[16]. These methods are the most common classifiers to determine the AMC based on the extracted features. However, these machine learning (ML)-based methods are locally optimum and lead to poor performance.

In recent years, the deep learning (DL) methods have received much attention due to promising results in a variety of fields, including computer vision [17], emotion analysis [18], and speech recognition [19]. Also, they are used for processing and analyzing information [20], as well as wireless communications [21]. It is important to note that some engineers have successfully used the DL to complete AMC tasks.

In [22], for the first time, O'Shea et al. introduced the idea of using the DL to classify ten modulation types by the convolutional neural network (CNN). The results have shown more accuracy with low SNR and more flexibility in detection than traditional methods. In [23], Residual Networks (ResNet) have recognized 24 modulations and have significantly improved the classification accuracy. In that paper, the neural network is combined with the baseband signal pre-processing method for feature extraction. Yashashwi et al. [24] have built and trained a CNN module for signal distortion correction to remove the impact of phase offset and random frequency. The carrier frequency offset (CFO) and the phase offset (PO) of the received signals are estimated by an artificial neural network (ANN) to eliminate the CFO and the PO effects.

A robust AMC method was also presented to identify three types of modulation signals [25]. The

simulation results have proved that this CNN-based method consumes less memory and is more robust to SNR changes than the conventional methods [25]. In order to detect the modulation types using a CNN-based model, the preprocessing technique was introduced in OFDM systems with phase shift, and the SNR was also estimated in [26]. The researchers have used in-phase and quadrature (IQ) samples to train the CNN as input. In this method, the bad effects of PO in OFDM systems are removed, then the classification with high accuracy is obtained.

On the other hand, Peng et al. [27] have employed two pre-trained models (e.g., the AlexNet and the GoogLeNet) to produce grid-like topologies in the images. They are used for the AMC. When employing feature fusion to improve performance, these are only relevant to the signal model of white Gaussian noise, which has many time-frequency transformations [28].

Even though all of these methods modify the AMC performance and reduce well-researched image identification challenges, they require complex image processing steps. In fact, the long short-term memory (LSTM) is adept at identifying the recurring patterns in long-term datasets. The LSTM network was trained by Rajendran et al. [29] using the received signals' amplitude and phase information and the recognition accuracy at SNR above 0 dB was approximately 90%. However, the spatial features of the signals are not taken into calculation.

Recently, in [30], a combination of the ResNet and the LSTM has been presented for the AMC. This method has achieved 92% accuracy. It is noteworthy that the ResNet has increased the complexity of the architecture. In [31], to decrease its complexity, a lightweight complex-valued residual network (CVResNet) has been introduced. Nonetheless, the accuracy rate is reduced, too.

This paper proposes a fast AMC technique based on HDNN named the CNN-LSTM, which combines the benefits of both the CNN and the LSTM. In comparison with [30]-[31], our proposed technique not only reduced the complexity of the CNN, but also increased the accuracy rate. The two-dimensional data are extracted from the modulated signals using the STFT method. Next, the spectrogram images are sent into the HDNN algorithm to obtain the modulation type of the signals. The simulation results have shown that the combination of the CNN and LSTM gives excellent results for a wide range of SNR (i.e., 0 - 25 dB). In fact, the proposed method has a significant reduction in the training time with negligible accuracy deterioration.

Modulation types for AMC are presented in Section 2. The proposed method called STFT-HDNN for classification is given in detail in Section 3. Section 4 presents the research findings. Finally, Section 5 summarizes the results and suggestions for future research.

II. DIGITAL MODULATION TECHNIQUE

The digital modulation provides a desired level of data security while it increases information.

Table I. Differences between ASK, PSK, and FSK Modulation Techniques.

Parameter	**ASK**	**PSK**	**FSK**
Modulation Types	Amplitude Shift Keying	Phase Shift Keying	Frequency Shift Keying
Modulation Equations	$X_{m_{ASK}}(t)=A_m \cos w_c t$	$X_{m_{PSK}}(t)=A\cos(w_c t+\theta_m)$	$X_{m_{FSK}}(t)=A\cos(w_c t)$
Carrier Signal	Amplitude is varied for binary representation 1 or 0	Phase is varied for binary representation 1 or 0	Frequency is varied for binary representation 1 or 0
Advantage	Simplicity	Fewer errors than ASK; Possibility to use a higher data rate than FSK	-Fewer errors than ASK
Disadvantage	It is more affected by noise.	The signal recovery process is more complex than ASK and FSK.	2*Spectrum of ASK
Application	Transmit digital data over optical fiber	radio communication system	Wireless transmission, high-frequency audio lines. etc.

capacity with a faster system and higher connection quality. They are more widely used than analog modulation due to their ability to transmit more information.

There are many digital modulation techniques. A digital baseband conversion is referred to a band-limited high-frequency passband signal that is used in digital transmission. The fundamental modulation methods are the ASK, FSK, and PSK that are used in the transition bands. The equations of these types with their advantages and disadvantages are shown in Table I.

The amplitude, frequency, or phase of the carrier can be changed between two or more different values to provide multi-level transmission. Also, it is possible to improve the data transmission throughput by using multiple carriers. In binary information transmission, a group of bits is often assigned to its own unique carrier. This transmission carrier has provided the information represented by the bit set. The QASK, QFSK, and QPSK modulations are commonly utilized in multiple-level modulation [32].

These modulations transmit two bits simultaneously. Thus, it doubles the transmission speed. The 8, 16, or 32 carriers increase the data transfer rate. Moreover, increasing the number of carriers increases the complexity of signal demodulation.

III. THE PROPOSED HDNN MODEL

In this section, we present our proposed method for fast classification of the modulation signals in the presence of noise. First, the modulation signals are converted into two-dimensional images by the STFT to obtain the time-frequency information. Secondly, this information is fed into the HDNN model as input data for classifying the modulation signals. To verify the results, it is applied to a classifier of basic digital modulation signals including ASK, FSK, PSK, QASK, QFSK, and QPSK. In

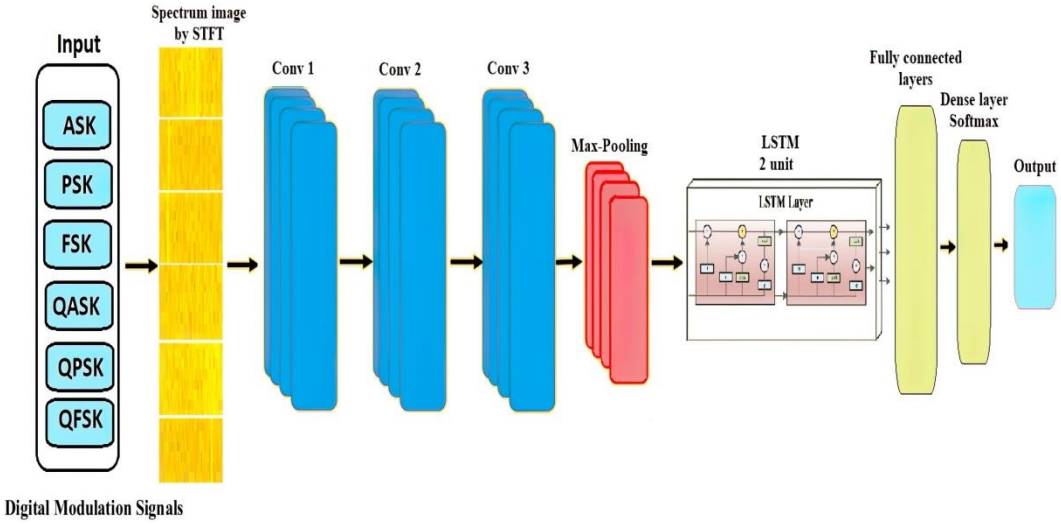

Fig. 1. Diagram of the proposed method.

In Fig. 1, a schematic diagram of the proposed method is shown

A. Short-Time Fourier Transform (STFT)

The STFT is a Fourier-associated transform utilized to find the sinusoidal frequency and phase content from the local signal sections as the signal changes over time. One of the common applications of the STFT is audio signal analysis [33]. There are two steps in the STFT: first, the temporal signals are segmented into equal lengths. Secondly, the Fourier transform is applied to each of these segments to obtain the time-frequency information in the form of a time-varying spectrogram as a function [34]. This means obtaining a time-frequency dilation instead of a Fourier transform model. The spectrogram extracted from STFT in continuous time can be written as equation (1).

$$S(t,f)=\int_{-\infty}^{+\infty} s(t).w(t-\tau).e^{-j\pi/\tau}d\tau. \tag{1}$$

where the window is controlled by the variable τ in (1) which shifts the window using the s(t) waveform. The w(t − τ) is the window function.

The STFT algorithm relies on the selection of the proper window. The frequency resolution of a rectangular window is lower than a triangular window. Because it decreases the frequency range. In the STFT, the window's width is reduced to increase the visibility of the time axis. In this instance, the frequency axis is decreased [35]-[36].

Discrete-time signals are often divided into equal overlapping frames. Then, a Fourier transform is performed on these frames [37]. Therefore, as shown in equation (2), a matrix is created that gets the phase and magnitude of points in time and frequency.

$$S(\tau,k)=\sum_{n-1}^{N} s[n].w[n-\tau].e^{-jnk} \tag{2}$$

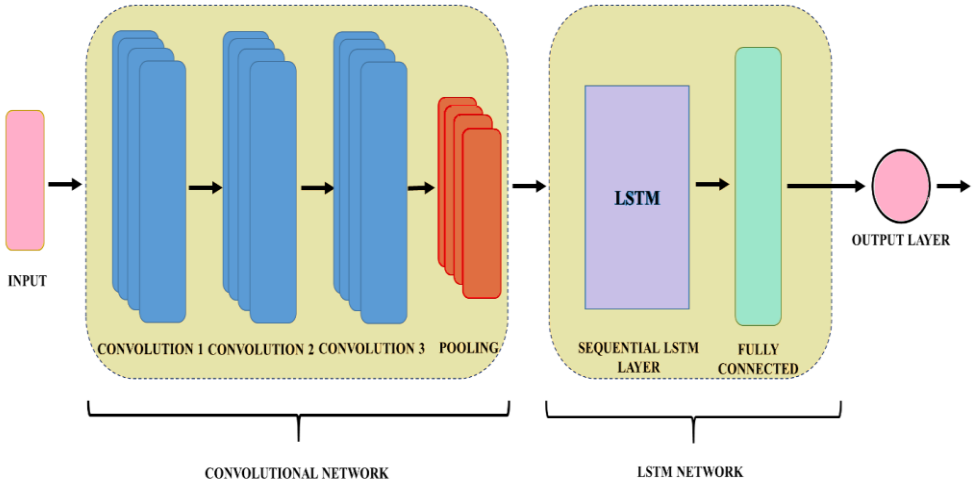

Fig. 2. Diagram of the proposed CNN-LSTM classification

where w(n) and s(n) denote the window function of length n and the converted signal. Therefore, the quadratic STFT takes the linear spectrogram as equation (3).

$$S_p(\tau,k) = |S(\tau,k)|^2 \tag{3}$$

B. Proposed HDNN for classification

In this paper, we describe a fast automatic signal modulation classification based on the HDNN. It combines the benefits of the CNN and LSTM networks. The speed and accuracy of AMC are critical for many applications. Thus, the combination of CNN and LSTM increases classification efficiency. Because CNN networks extract spatial features of the input information well and classify quickly. In addition, LSTM networks capture sequence data to extract temporal features accurately. Therefore, classification accuracy is increased. Fig. 2 displays the architecture of our proposed CNN-LSTM for AMC.

A convolutional neural network (CNN) is a type of artificial neural network including a set of sequential and deep feed-forward layers [38]. These layers produce local features of the input information [39]. Most of these layers are followed by the pooling layer, which contributes to capturing relevant local features and reduces computational complexity. Rectified Linear Unit (ReLU) is embedded between these layers as an activation function which can make network training more efficient. These networks also contain fully connected layers which include a softmax regression layer to obtain the desired classification. Backpropagation algorithms are used to train CNNs with cost minimization based on weights (W) as equation (4).

$$L = -\frac{1}{|X|}\sum_{i}^{|X|} ln\,(p(y^i|X^i)) \tag{4}$$

where, $|X|$ is the number of training data, X^i is the i^{th} training data with the label corresponding to y^i, and $(p(y^i|X^i)$ points out the probability which accurately shows X^i matching.

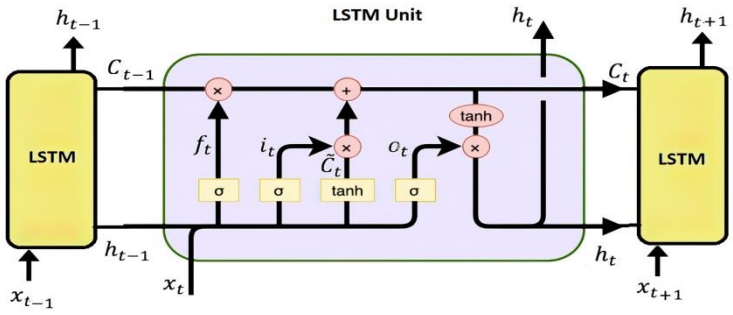

Fig. 3. Structure of the basic LSTM.

The LSTM model has achieved high classification accuracy for many applications and a wide range of modulation signals [40]. It is a common type of recurrent neural network (RNN), but its architecture contains special gates that help improve the vanishing gradient problem [41]. The architecture of LSTM possesses a short-term memory of RNN that can persist for a vast number of time steps. It means "long short-term memory" [42]. Linking the previous and current state of the LSTM increases its ability to learn temporal data. Fig. 3 illustrates the structure of the basic LSTM. A memory cell can store information for long periods, and the gates regulate data flow into and out of the cell. Whereas the input gate is responsible for defining the new information of the current state, the forget gate determines which information of the previous state should be stored or discarded. The output gates control the current state information.

Since the output gate information retains useful long-term dependencies, the LSTM network makes predictions about the current and future steps. The mathematical equations for the LSTM network gates are given in equations (5-9).

$$f_t = \sigma(W\ [x_t, h_{t-1}, C_{t-1}] + b_t) \tag{5}$$

$$i_t = \sigma\,(W\ [x_t, h_{t-1}, C_{t-1}] + b_i) \tag{6}$$

$$O_t = \sigma\,(W\ [x_t, h_{t-1}, C_t] + b_o) \tag{7}$$

$$C_t = f_t \times C_{t-1} + i_t \times \tanh(W\ [x_t, h_{t-1}, C_{t-1}] + b_c) \tag{8}$$

$$h_i = \tanh(Ct) \times o_t \tag{9}$$

where f_t, i_t, and O_t are the activation vectors of the forget, input, and output gates, respectively. x_t refers to the input vector. The weight vector is W, and the bias vector is b. h_t is the output of the LSTM unit, and h_{t-1} is the output of the previous cell. C_t is the cell state, and C_{t-1} shows memory for the previous cell. σ is the sigmoid function.

The CNN-LSTM based on the STFT algorithm is the basis of our proposed AMC technique. An innovative approach to the classification of six modulation signals with 0-25 dB noise levels ranging is presented in this research. Modulation methods encode data from 1 to 255. These modulated signals are fed to the STFT for obtaining the time-frequency information as the HDNN input.

Then, the recovered time-frequency data are fed into the CNN, LSTM, and fully connected layers (i.e., HDNN method), respectively. The steps of our proposed strategy are shown in Fig. 1. The input signal (time-frequency) is processed by several convolutional layers. In this design, three convolutional layers with 256 feature maps are employed. The dimension of these convolutional layers is 9 * 9, 4 * 3, and 4 * 3, respectively. We use a non-overlapping maximum pooling technique and apply frequency pooling. The size of the pooling layer is 3*3.

Then, the LSTM layers are applied. It is ideal for time series modeling. They take the CNN output and apply it as the input data. In fact, we used two LSTM layers with 832 cells and a 512-unit projection layer to reduce the size of the final model.

CNN has advantages such as learning local features, transformation invariance of input data, and weight-sharing. However, it has limitations such as the problem of vanishing gradients. Therefore, in this paper, we have used the LSTM to solve the above problem because it has memory and it does not require a previous length of the input data. Thus, using the two networks together increases the accuracy of the proposed method in automatically classifying modulation signals due to its ability to obtain temporal and spatial features from the input information.

IV. EXPERIMENTAL RESULTS

This paper has explained a digital modulation classification system using hybrid STFT and CNN-LSTM approach. Decimal data from 1 to 255 are encoded in six modulated types with noise levels (0 - 25 dB). Fig. 4 shows the graphical Matlab simulations of the modulation types (e.g., ASK, PSK, FSK, QASK, QASK, and QASK) with different SNR rates and 5 dB increments.

The result is 255*6 samples. Using the STFT technique, 9180 images are obtained as the spectrum diagram representing the time-frequency information. Fig. 5 shows graphical simulations for spectrum images extracted from modulation signals by the STFT algorithm.

For the proposed digital modulation classification, two experiments are configured: First, we have considered the success of our proposed method in classifying the modulated signals with a 5 dB SNR value, where 255 samples were classified for each category. In the second test, 1530 samples from each category have an SNR ranging from 0-25 dB. As a result, the proposed HDNN is fed with 9180 spectrum images obtained from standard STFT, and these images are automatically cropped to remove undesirable white regions for increasing accuracy. Then, the spectrum images as time-frequency information are used as input for the proposed classification network (i.e., HDNN). All experiments took place on a computer equipped with MATLAB (2021a) as well as an NVIDIA GeForce GTX 1660Ti graphics card with 16 GB of RAM.

The HDNN model is fed total data from 1530 spectrogram images for each class. To classify the modulation signals, the data are randomly split into 70% and 30 % for training and testing,

respectively. We have used a confusion matrix to quantify the model's performance for the digital AMC challenge. Here, this matrix has a diagonal pattern for recognizing modulation types. It emphasizes a high degree of categorization accuracy of the model. The results are shown in Fig. 6.

In Table II and Table III, the experiment's outcomes are summarized. As we have seen, the overall accuracy of all SNRs is above 99%. This confirms that the suggested technique is robust against background noise. To determine the effectiveness of our method, we have utilized the recall, precision, accuracy, and F1-score metrics, as shown in (10), (11), (12), and (13) [43].

$$Recall = \left(\frac{true\ positive}{true\ positive + false\ Negative} \right)_{for\ i^{th} class} \tag{10}$$

$$Precision = \left(\frac{true\ positive}{true\ positive + false\ positive} \right)_{for\ i^{th} class} \tag{11}$$

$$Accuracy = \left(\frac{total\ number\ of\ correct\ samples}{number\ of\ total\ sample} \right)_{for\ i^{th} class} \tag{12}$$

$$F1 - score = \left(2 \times \frac{precision \times recall}{precision + recall} \right)_{for\ i^{th} class} \tag{13}$$

These metrics have been obtained using false negative, true positive, true negative, and false positive indices. The suggested approach's overall accuracy, recall, precision, and F1-score are 99.92%, 99.87%, 99.87%, and 99.87%, respectively. Nonetheless, the FSK is the worst-classified modulation type with 99.7% accuracy.

The results of the experiment have validated the efficacy of the suggested strategy for the modulation categorization task. Depending on the STFT with the CNN-LSTM, we have developed a hybrid method to categorize digital modulation types. We have used the STFT which generates spectrograms as our data source. It is possible to use several different window functions, such as Hamming or Hann.

Finally, we have compared the proposed technique to various pre-trained CNN-based models for digital modulation categorization. We have used VGG-16, GoogLeNet, VGG-19, ResNet-101, and AlexNet to compare our proposed model. These models' architecture is not considered in this study. They just had the default parameters to train and test. Results are shown in Table IV. with various performance metrics. Generally, the CNN models have obtained a high classification accuracy (more than 99 percent accuracy). ResNet-101 training has lasted an average of 917 minutes. The VGG-19, GoogleNet, and VGG-19 were tested for over an hour. The elapsed time is illustrated in Table IV and Fig. 7. They make it easy to demonstrate that ours is more rapid than other methods with a negligible decrease in AMC accuracy over a wide range of SNRs. In fact, the reduction in processing time was predictable and expectable. Because other networks are more complicated than our proposed network.

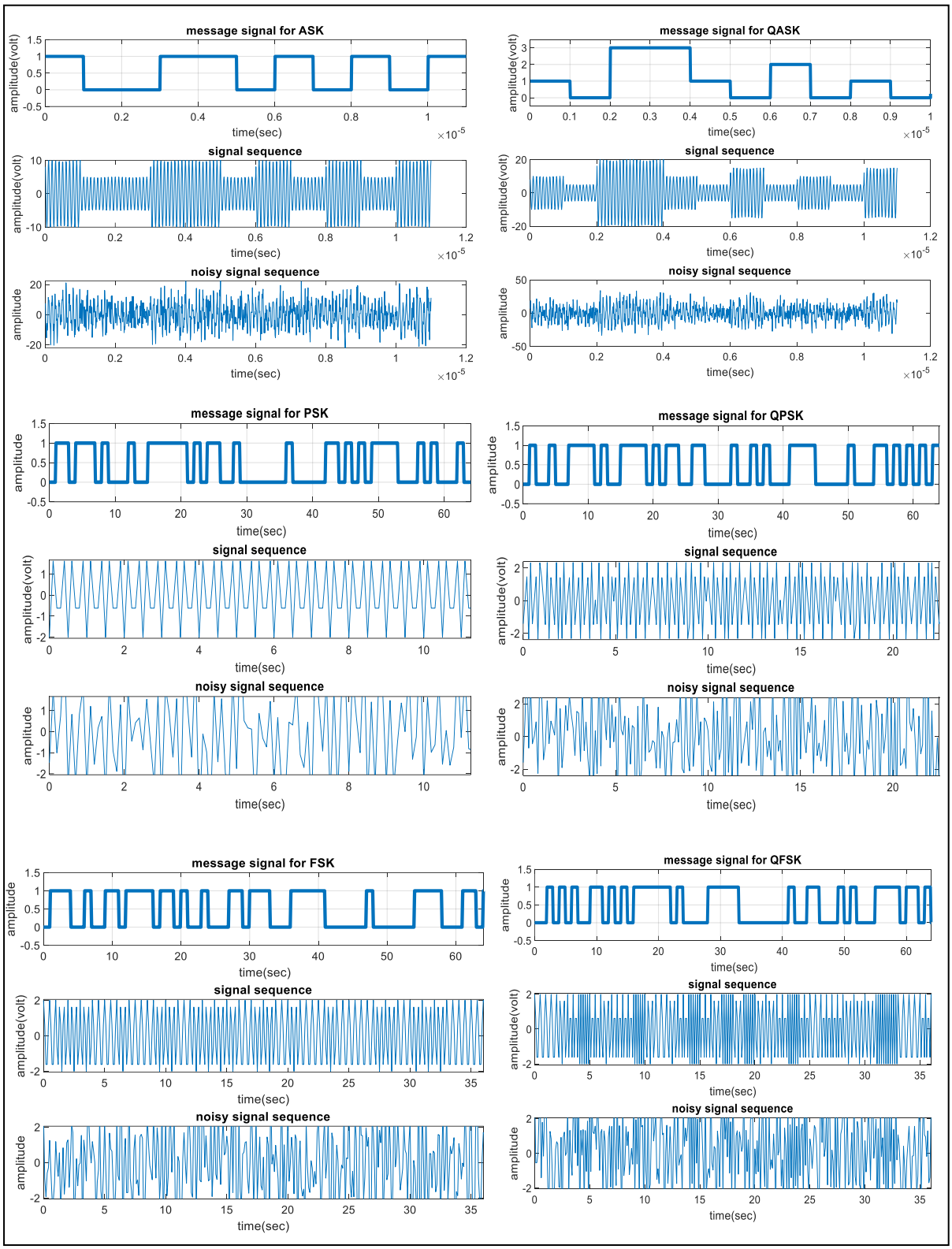

Fig. 4. The graphical simulations for data of 10110100 from six modulation signals with 5 dB.

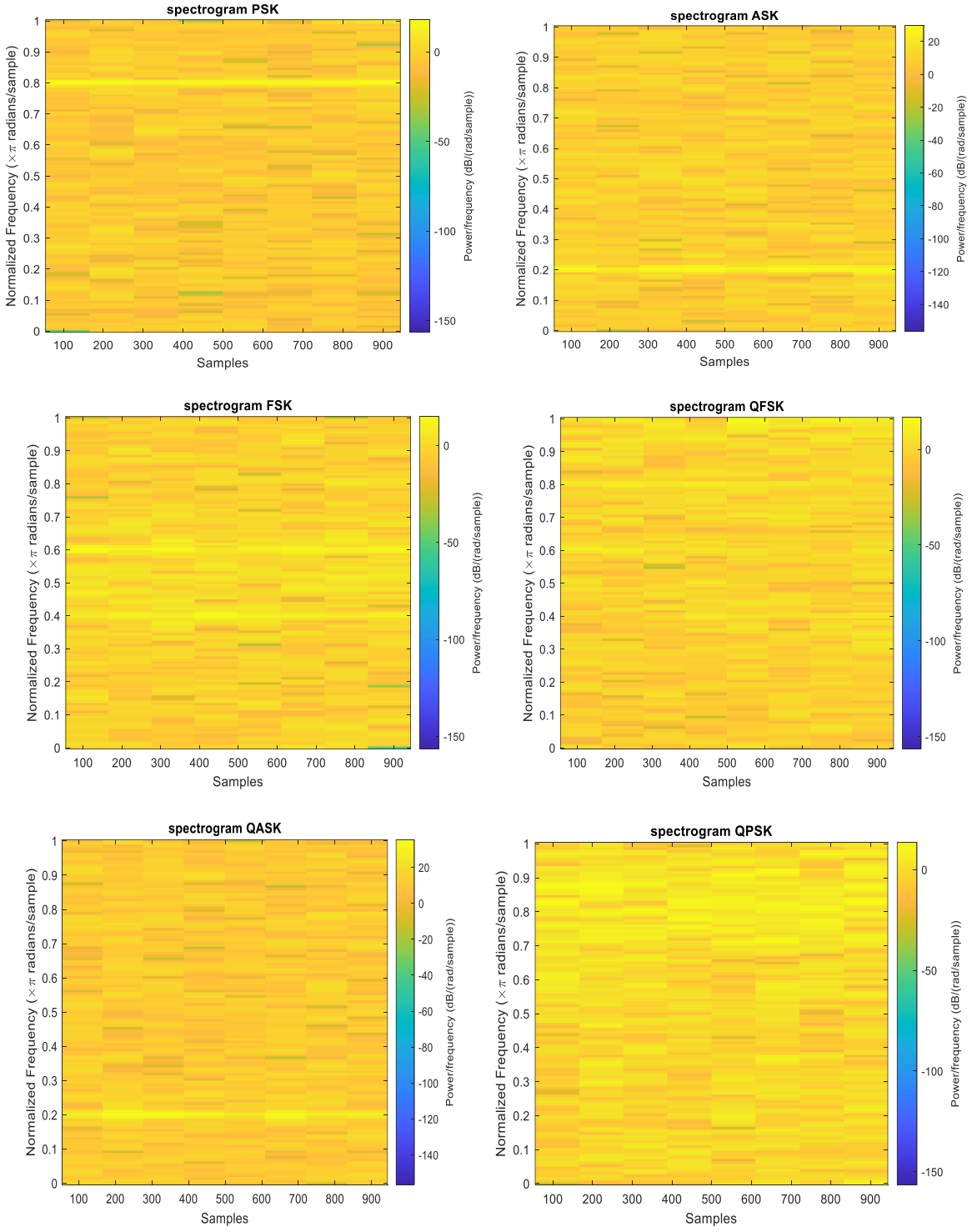

Fig. 5. The graphical simulations for spectrum images extracted from modulation signals by the STFT algorithm.

In addition, we have fed effective and meaningful features to the network. Furthermore, the results obtained from various metrics are shown in Fig. 8 and Fig. 9.

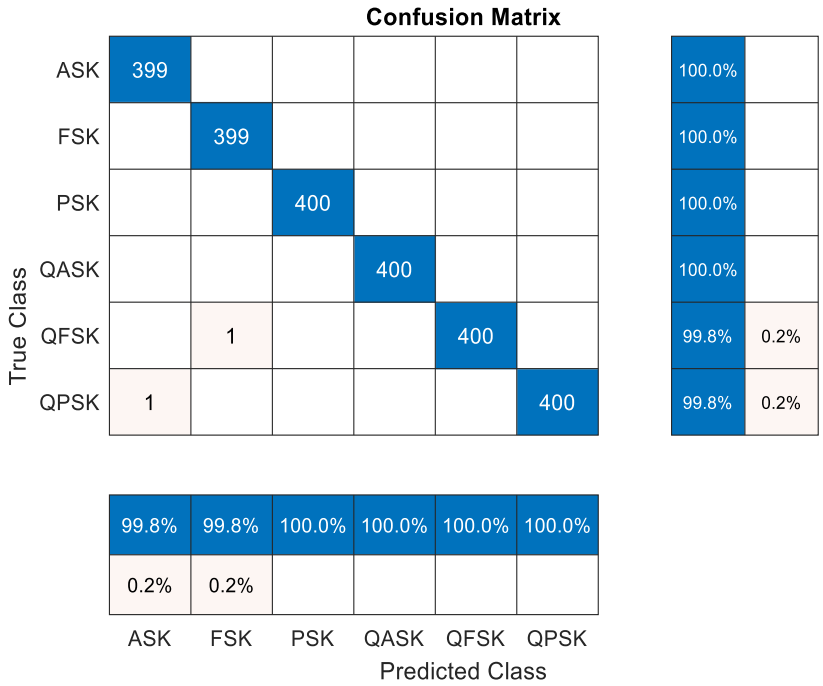

Fig. 6. Categorization outcomes due to the confusion matrix.

Table II. Accuracy of the proposed method with different SNR rates.

Classes	**SNR (dB)**						
	0	5	10	15	20	25	Average accuracy
ASK(Ours)	99.8%	99.8%	99.9%	99.9%	99.9%	99.9%	99.86%
FSK(Ours)	99.5%	99.5%	99.7%	99.9%	99.9%	99.9%	99.7%
PSK(Ours)	100%	100%	100%	100%	100%	100%	100%
QASK (Ours)	100%	100%	100%	100%	100%	100%	100%
QFSK (Ours)	100%	100%	100%	100%	100%	100%	100%
QPSK (Ours)	100%	100%	100%	100%	100%	100%	100%
Average accuracy (Ours)	99.9%	99.9%	99.9%	99.9%	99.9%	99.9%	99.926%

Table III. The results of the proposed method with all SNR rates in classes.

Classes	**Acc.**	**Precision**	**Recall**	**F1 score**
ASK(Ours)	99.86%	99.75%	100%	99.875%
FSK (Ours)	99.7%	99.5%	100%	99.749%
PSK (Ours)	100%	100%	100%	100%
QASK (Ours)	100%	100%	100%	100%
QFSK (Ours)	100%	100%	99.502%	99.751%
QPSK (Proposed)	100%	100%	99.751%	99.875%
Average (Ours)	99.926%	99.875%	99.8755%	99.875%

Table IV. The results of our proposed approach and several CNN models for AMC.

Metrics	AlexNet	VGG16	VGG19	Googlenet	ResNet101	Proposed
Acc.	0.9939	1	0.9989	0.9956	1	0.99926
Precision	0.9940	1	1	0.9978	1	0.99875
Recall	0.9939	1	0.9989	0.9967	1	0.998755
F1 score	0.9939	1	0.9995	0.9973	1	0.99875
Time(min)	27.3	206.1	240.3	217.5	917.4	1.5

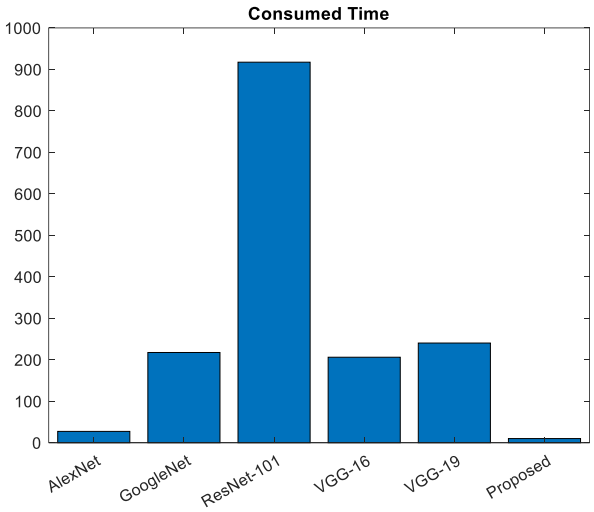

Fig. 7. Comparison of training time between our proposed model and other CNN models.

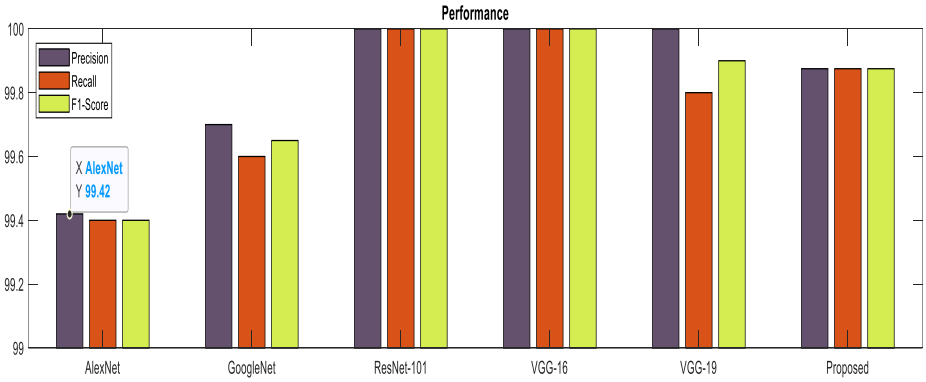

Fig. 8. Performance of our proposed model and other pre-trained models.

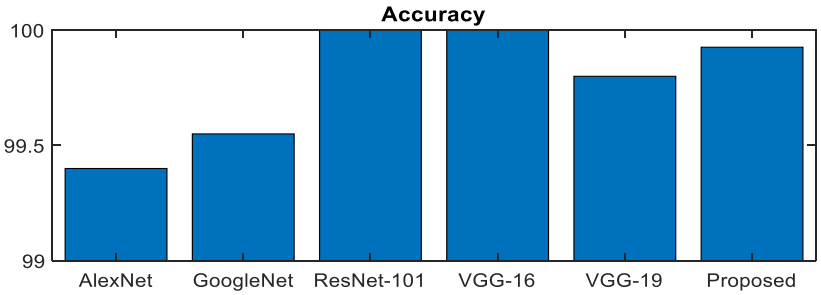

Fig. 9. Accuracy of our proposed model and other pre-trained models.

V. CONCLUSION

Recent deep-learning networks have been utilized in the AMC issue. This paper has introduced the HDNN method for an automatic classification task based on spectrograph images. Initially, the transfer learning approach is employed to test the method's robustness in a range of SNR values (from 0 to twenty-five dB) with six types of modulated signals. According to the results, we have concluded that our model is able to correctly classify different types of modification. In other words, the experimental results have shown that the proposed HDNN model can determine the types of modulation well. The classification accuracy of the proposed method is more than 99% for all types of signals with different SNR values. On the other hand, the performance of the proposed model has been compared with other CNN methods, such as VGG-19, GoogleNet, ResNet 101, and VGG-16, in the AMC task. It was found that the proposed method has outperformed all other methods in terms of efficiency and training speed. The training time of the proposed method was 1.5 min. Since the AMC is very important for classifying signals in communications systems, we can concatenate other networks for the AMC task in the future.

REFERENCES

[1] X. Hao and *et al*., "Automatic Modulation Classification via Meta-Learning," *IEEE Internet of Things Journal*, vol. 10, no. 14, pp. 12276-12292, July 2023.

[2] C. Lin, W. Yan, L. Zhang, and W. Wang, "A real-time modulation recognition system based on software-defined radio and multi-skip residual neural network," *IEEE Access*, vol. 8, pp. 221235–221245, Dec. 2020.

[3] B. Ramkumar, "Automatic modulation classification for cognitive radios using cyclic feature detection," *IEEE Circuits and Systems Magazine*, vol. 9, no. 2, pp. 27–45, June 2009.

[4] Q. Zheng, X. Tian, Z. Yu, H. Wang, A. Elhanashi, and S. Saponara, "DL-PR: Generalized automatic modulation classification method based on deep learning with priori regularization," *Eng. Appl. Artif. Intell.*, vol. 122, p. 106082, June 2023.

[5] H. Tayakout, I. Dayoub, K. Ghanem, and H. Bousbia-Salah, "Automatic modulation classification for D-STBC cooperative relaying networks," *IEEE Wirel. Commun. Lett*., vol. 7, no. 5, pp. 780–783, April 2018.

[6] S. Huang, C. Lin, K. Zhou, Y. Yao, H. Lu, and F. Zhu, "Identifying physical-layer attacks for IoT security: An automatic modulation classification approach using multi-module fusion neural network," *Phys. Commun.*, vol. 43, pp. 1–10, Dec. 2020.

[7] J. Zheng and Y. Lv, "Likelihood-based automatic modulation classification in OFDM with index modulation," *IEEE Trans. Veh. Technol*., vol. 67, no. 9, pp. 8192–8204, Sept. 2018.

[8] A. Kumar, S. Majhi, G. Gui, H. C. Wu, and C. Yuen, "A Survey of Blind Modulation Classification Techniques for OFDM Signals," *Sensors*, vol. 22, no. 3, pp. 1–32, Jan. 2022.

[9] L. Xie and Q. Wan, "Cyclic Feature-Based Modulation Recognition Using Compressive Sensing," *IEEE Wirel. Commun. Lett.*, vol. 6, no. 3, pp. 402–405, June 2017.

[10] L. Han, F. Gao, Z. Li, and O. A. Dobre, "Low Complexity Automatic Modulation Classification Based on Order-Statistics," *IEEE Trans. Wirel. Commun*., vol. 16, no. 1, pp. 400–411, Jan. 2017.

[11] R. Gupta, S. Majhi, and O. A. Dobre, "Design and Implementation of a Tree-Based Blind Modulation Classification Algorithm for Multiple-Antenna Systems," *IEEE Trans. Instrum. Meas*., vol. 68, no. 8, pp. 3020–3031, Aug. 2019.

[12] R. Gupta, S. Kumar, and S. Majhi, "Blind Modulation Classification for Asynchronous OFDM Systems over Unknown Signal Parameters and Channel Statistics," *IEEE Trans. Veh. Technol.*, vol. 69, no. 5, pp. 5281–5292, May 2020.

[13] K. Triantafyllakis, M. Surligas, G. Vardakis, and S. Papadakis, "Phasma: An automatic modulation classification system based on Random Forest," *In 2017 IEEE Int. Symp. Dyn. Spectr. Access Networks (DySPAN),* pp. 1-3, March 2017.

[14] H. Tayakout, F. Z. Bouchibane, and E. Boutellaa, "On the Performance of Digital Modulation Classification for Cooperative Multiple Relays Network System without Direct Channel," *in 2022 2nd International Conference on Advanced Electrical Engineering (ICAEE),* pp. 1–5, Oct. 2022.

[15] W. Zhang, "Automatic modulation classification based on statistical features and Support Vector Machine," *2014 31th URSI Gen. Assem. Sci. Symp. URSI GASS 2014*, no. 2, pp. 1–4, Aug. 2014.

[16] M. O. Mughal and S. Kim, "Signal classification and jamming detection in wide-band radios using naïve bayes classifier," *IEEE Commun. Lett*., vol. 22, no. 7, pp. 1398–1401, July 2018.

[17] O. Russakovsky, and *et al.*, "ImageNet Large Scale Visual Recognition Challenge," *Int. J. Comput. Vis.*, vol. 115, no. 3, pp. 211–252, April 2015.

[18] C. Gan, L. Wang, and Z. Zhang, "Multi-entity sentiment analysis using self-attention based hierarchical dilated convolutional neural network," *Futur. Gener. Comput. Syst.*, vol. 112, pp. 116–125, Nov. 2020.

[19] H. Mohana and M. Suriakala, "An Enhanced Prospective Jaccard Similarity Measure (PJSM) to Calculate the User Similarity Score Set for E-Commerce Recommender System," *In Intelligent System Design: Proceedings of Intelligent System Design: INDIA 2019*, vol. 1171 pp. 129–142, Aug. 2021.

[20] C. Luo, K. Zhang, S. Salinas, and P. Li, "SecFact: Secure Large-scale QR and LU Factorizations," *IEEE Trans. Big Data*, vol. 7, no. 4, pp. 796–807, Oct. 2021.

[21] H. Ye, L. Liang, G. Y. Li, and B.-H. Juang, "Deep Learning-Based End-to-End Wireless Communication Systems With Conditional GANs as Unknown Channels," *IEEE Trans. Wirel. Commun.*, vol. 19, no. 5, pp. 3133–3143, May 2020.

[22] T. J. O'Shea, J. Corgan, and T. C. Clancy, "Convolutional radio modulation recognition networks," *Commun. Comput. Inf. Sci.*, vol. 629, pp. 213–226, Aug. 2016.

[23] T. J. O'Shea, T. Roy, and T. C. Clancy, "Over-the-Air Deep Learning Based Radio Signal Classification," *IEEE J. Sel. Top. Signal Process.*, vol. 12, no. 1, pp. 168–179, Feb. 2018.

[24] K. Yashashwi, A. Sethi, and P. Chaporkar, "A Learnable Distortion Correction Module for Modulation Recognition," *IEEE Wirel. Commun. Lett.*, vol. 8, no. 1, pp. 77–80, Feb. 2019.

[25] T. Zhang, C. Shuai, and Y. Zhou, "Deep Learning for Robust Automatic Modulation Recognition Method for IoT Applications," *IEEE Access*, vol. 8, pp. 117689–117697, March 2020.

[26] J. Shi, S. Hong, C. Cai, Y. Wang, H. Huang, and G. Gui, "Deep Learning-Based Automatic Modulation Recognition Method in the Presence of Phase Offset," *IEEE Access*, vol. 8, pp. 42831–42847, March 2020.

[27] S. Peng and *et al.*, "Modulation Classification Based on Signal Constellation Diagrams and Deep Learning," *IEEE Trans. Neural Networks Learn. Syst*., vol. 30, no. 3, pp. 718–727, July 2018.

[28] C. Hou, Y. Li, X. Chen, and J. Zhang, "Automatic modulation classification using KELM with joint features of CNN and LBP," *Phys. Commun.*, vol. 45, p. 101259, April 2021.

[29] S. Rajendran, W. Meert, D. Giustiniano, V. Lenders, and S. Pollin, "Deep learning models for wireless signal classification with distributed low-cost spectrum sensors," *IEEE Trans. Cogn. Commun. Netw.*, vol. 4, no. 3, pp. 433–445, May 2018.

[30] M. M. Elsagheer and S. M. Ramzy, "A hybrid model for automatic modulation classification based on residual neural networks and long short term memory," *Alexandria Engineering Journal*, vol. 67, pp. 117-128, March 2023.

[31] F. Wang, T. Shang, C. Hu, and Q. Liu, "Automatic Modulation Classification Using Hybrid Data Augmentation and Lightweight Neural Network," *Sensors*, vol. 23, no. 9, p. 4187, April 2023.

[32] R. G. Gallager, *Principles of digital communication*, Cambridge, UK: Cambridge University Press, 2008.

[33] R. He, Q. Chen, and W. He, "Study on compressed sensing imaging based on intensity modulation in Fourier domain," *Optik*, vol. 125, no. 14, pp. 3759-3763, July 2014.

[34] L. Zhou, Z. Sun, and W. Wang, "Learning to short-time Fourier transform in spectrum sensing." *Physical Communication*, vol. 25, pp. 420-425, Dec. 2017.

[35] J. L. Semmlow, *Biosignal and Medical Image Processing*, CRC press, Oct. 2004.

[36] Ö. F. Alçin, S. Siuly, V. Bajaj, Y. Guo, A. Şengür, and Y. Zhang, "Multi category EEG signal classification developing time-frequency texture features-based Fisher vector encoding method," *Neurocomputing*, vol. 218, pp. 251-258, Dec. 2016.

[37] N. Daldal, Z. Cömert, and K. Polat, "Automatic determination of digital modulation types with different noises using Convolutional Neural Network based on time–frequency information," *Applied Soft Computing Journal*, vol. 86, p. 105834, Jan. 2020.

[38] C. Du, S. Gao, Y. Liu, and B. Gao, "Multi-focus image fusion using deep support value convolutional neural network," *Optik*, vol. 176, pp. 567–578, Jan. 2019.

[39] Z. Zhao, Y. Zhang, Z. Comert, and Y. Deng, "Computer-Aided Diagnosis System of Fetal Hypoxia Incorporating Recurrence Plot With Convolutional Neural Network," *Frontiers in physiology*, vol. 10, pp. 1–14, March 2019.

[40] R. Zhou, F. Liu, and C. W. Gravelle, "Deep Learning for Modulation Recognition: A Survey with a Demonstration," *IEEE Access*, vol. 8, pp. 67366–67376, April 2020.

[41] I. H. Sarker, "Deep Learning: A Comprehensive Overview on Techniques, Taxonomy, Applications and Research Directions," *SN Comput. Sci*., vol. 2, no. 6, pp. 1–20, Aug. 2021.

[42] S. Hochreiter and J. Schmidhuber, "Long Short-Term Memory," *Neural Comput*., vol. 9, no. 8, pp. 1735–1780, Nov. 1997.

[43] C. Nicholson, Evaluation metrics for machine learning—Accuracy, precision, recall, and F1 defined, https://wiki.pathmind.com/accuracy-precision-recall-f1 (2019). Accessed Nov. 2023.